Shin *et al. Micro and Nano Systems Letters* (2021) 9:15
https://doi.org/10.1186/s40486-021-00137-0

Micro and Nano Systems Letters

LETTER

Open Access

Micro multi-nozzle jet coating of organic thin film for organic light-emitting diode lighting devices

Kwon-Yong Shin[1], Mingyu Kang[2], Kwan Hyun Cho[1], Kyung-Tae Kang[1] and Sang-Ho Lee[1*]

Abstract

Uniform deposition across large areas of an organic layer is one of the challenges for the industrial application of solution-based organic light-emitting diode (OLED). In this paper, we propose an organic thin film deposition method for OLED using a micro multi-nozzle jet coating process. The developed micro multi-nozzle jet head consists of eighteen nozzles (100 μm diameter), a side suction line, inlets, and a nozzle protection outer hole. To demonstrate organic thin film deposition for OLED lighting device fabrication, a poly(3,4-ethylenedioxythiophene):poly(styrene sulfonate) (PEDOT:PSS) solution was used as a hole injection layer (HIL). Thickness uniformity of the PEDOT:PSS thin film was analyzed by regulating the jetting pressure. Through single-path coating of twelve successive stable column-jet flows, PEDOT:PSS organic film of 26 mm width was coated on an ITO substrate at 1 m/s head speed. The PEDOT:PSS thin film of 24.25 ± 1.55 nm (CV = 6.39%) thickness was obtained by the proposed coating method. For the feasibility test, OLED lighting devices with emission areas of 20 mm × 20 mm and 70 mm × 70 mm were successfully fabricated using PEDOT:PSS films deposited by a micro multi-nozzle jet coating method.

Keywords: Thin film, PEDOT:PSS, Multi-nozzle jet, Continuous flow, OLED, Coating

Introduction

Organic light-emitting diode (OLED) has received great attention due to their excellent characteristics including large-area emission, low power consumption, flexibility, and thin thickness in the lighting and display industries [1–3]. A vacuum thermal evaporation process is a commonly used process to form multi-layer architectures needed for OLEDs with high efficiency and a long lifetime. But, vacuum process-based manufacturing has demerits that require a huge investment for equipment and peripheral facilities. Although OLED has many advantages applicable to electronic products such as displays, lighting, and smart labels, its high manufacturing costs are one of the factors obstacles to entering various application markets. Recently, as an alternative technology to the vacuum thermal evaporation process, solution-based process technology is being considered as a process for reducing the manufacturing cost of OLED [4–8].

Various solution-based thin film deposition processes have been developed for OLED manufacturing and are divided into a printing process and a coating process. The representative printing process includes inkjet printing, gravure printing, flexo printing, and screen printing. In particular, inkjet printing is widely used as a patterning technology in the digital textile and electronic industries due to its characteristics such as a mask-less and simple process, non-contact approach, and a low-cost process with efficient material usage [9, 10]. The coating process involves spin coating, dip coating, knife coating, spray coating, slide coating, and slot die coating [1, 5, 11–17]. Spin coating is a common method for depositing organic thin films to substrates and slot-die coating is one of the

*Correspondence: sholee7@kitech.re.kr
[1] Korea Institute of Industrial Technology, 143 Hanggaul-ro, Sangnok-gu, Ansan-si, Gyeonggi-do 15588, Republic of Korea
Full list of author information is available at the end of the article

effective solutions to deposit a variety of organic solutions onto glass, stainless steel, and plastic substrates for large-area coating of organic thin films. Dainippon Screen and DuPont Displays Inc. have developed a multi-nozzle printing process for OLED patterning technology. For a solution-based manufacturing system, the multi-nozzle printing system can offer many advantages including a high yield and scalable printing process, a simple nozzle structure, and solution patterning, etc. The nozzle printing process uses a continuous stream jet flow that is ejected from nozzles and directly prints stripe patterns on the substrate with a high speed of above 1 m/s. The RGB pixel printing process for OLED display was demonstrated by moving a continuous liquid column back and forth on the substrate in alignment with the rows of patterned non-wetting lanes. The thickness profiles for emission layer films showed the good uniformity of ± 5% deviation for 38 nm on a 150 × 150-mm printed substrate [18–22]. OLED manufacturing cost using the multi-nozzle printing process and advanced materials is expected to be about 50% lower than that of the 4th Generation panel manufactured by the existing vacuum process [23]. Recently, inkjet printing technologies has been used in OLED thin-film encapsulation (TFE) and RGB pixel patterning. IHS Markit's report suggests that inkjet printing has the potential to save 15–25% production cost compared to the conventional OLED manufacturing method [24]. It was reported to print multiple user-controlled thicknesses in the sub-10 μm range within one single display subpanel to compensate for topology changes [25].

In our previous research, for the solution-based thin film deposition process, a micro multi-nozzle (μ-MN) jet head with a side suction function was developed to prevent the generation of an initial dangling droplet at the nozzle tip, which delays the formation time of a continuous stream jet flow. The continuous stream jet flow could be stably formed by the jetting pneumatic pressure within 1 s when vacuum pressure was applied to the side suction channel [26, 27]. Unlike other previous studies that demonstrated nozzle printing of RGB stripe pixel patterns for OLED display, our research objective is to develop a scalable multi-nozzle jet coating method for uniform organic thin film deposition for the solution-based large-area manufacturing of OLED lighting devices. The coating area was enlarged by adjusting the print pitch of the developed μ-MN jet head. To obtain a flat PEDOT:PSS thin film of less than 30 nm thickness, the jetting pneumatic pressure applied to the μ-MN jet head was optimized at 1 m/s stage speed through analysis of coating uniformity. An ITO-deposited glass substrate was exposed by an O_2 plasma to obtain a wetting surface before the coating process. OLED lighting device fabrication was successfully demonstrated by coating a PEDOT:PSS thin film as a hole injection layer (HIL). We also fabricated OLED lighting devices with a 70 mm × 70 mm emission area to investigate the large-area coating performance of a μ-MN jet coating method compared to a micro single-nozzle (μ-SN) jet coating method.

Experimental

Materials and coating process

A PEDOT:PSS (Clevios CH8000, Heraeus, Germany aqueous dispersion of 2.8 wt% was used to coat a hole injection layer (HIL) thin film for fabrication of the OLED lighting device. The pristine PEDOT:PSS was diluted with ethanol (EtOH) at a 90% volume ratio. The dilution ratio was chosen from the previous study results on the ink formulation of PEDOT:PSS for HIL deposition by single nozzle coating with a SUSS needle in an OLEDs structure [28]. The measured viscosity and the surface tension of the diluted PEDOT:PSS solution were 1.4 cP and 23.8 mN/m, respectively.

We used an indium tin oxide (ITO)-deposited square glass as the coating substrate. O_2 plasma system (JSPCS-300, JESAGIHANKOOK, Korea) was used to make the surface of the substrates have high wettability after wet cleaning. Nozzle jet coating of the diluted PEDOT:PSS solution was performed with a μ-MN jet coating system (Mini Streamjet Coater, DEVICEENG, Korea) (Fig. 1). The eighteen nozzles were grouped by six and divided into three groups. The grouped nozzles were connected to three ink supply lines and one side tube was connected to the suction channel. The diluted PEDOT:PSS solution was coated through twelve micro nozzles, and the system coating conditions were a μ-MN jet head moving

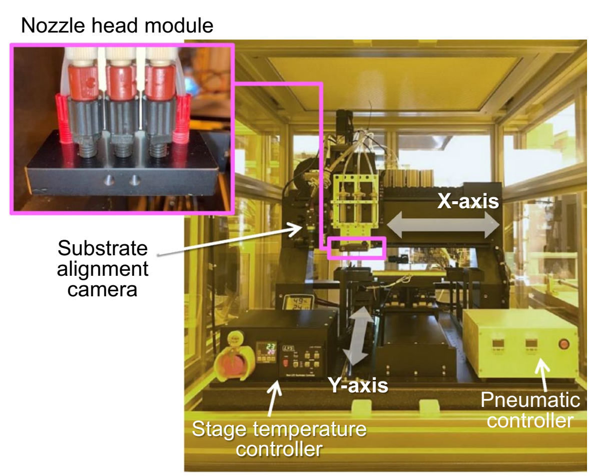

Fig. 1 Micro multi-nozzle jet coating system (Mini Streamjet Coater, DEVICEENG, Korea). The inset image shows an enlarged nozzle head module photograph

velocity (V_{head}) of 1 m/s, a gap distance between the nozzle head and substrate ($d_{head\text{-}subs}$) of ~1 mm, a head suction pressure($P_{suction}$) of 90 kPa, and a jetting pneumatic pressure ($P_{jetting}$) of 100~200 kPa. The coating process was carried out at 24 °C (±1.0 °C) and 50% (±5%) relative humidity.

Fabrication of OLED lighting device

An OLED lighting device with an emission area of 20 mm × 20 mm was fabricated by combining the μ-MN jet coating method and the vacuum deposition process. First, ITO-deposited (165 nm) glass substrate was sequentially cleaned by ultrasonic agitation in acetone and isopropyl alcohol for 30 min, and then dried with N_2 after deionized water rinsing. ITO was patterned by a wet etchant with a photoresist mask to form an anode electrode (Fig. 2a). The substrate was then treated by an O_2 plasma system for 30 s, and a PEDOT:PSS layer (HIL) was deposited by micro multi-nozzle jet coating (Fig. 2b). Shadow masking and a thermal vapor deposition process were performed to pattern 70 nm-thick N,N′-Di(1-naphthyl)-N,N′-diphenyl-(1,1′-biphenyl)-4,4′-diamine (NPB) as a hole transport layer, 30 nm-thick tris-(8-hydroxyquinoline)aluminum (Alq_3) as an emitting layer, 1 nm-thick lithium fluoride (LiF) as an electron transport layer and 100 nm-thick aluminum (Al) as a cathode (Fig. 2c–e). Thermal vapor deposition was operated under a vacuum of 3.6×10^{-7} Torr. For the encapsulation process, after dispensing UV resin to the edges of the glass lid, the resin was cured with UV light for 3 min (Fig. 2f). The entire process of the encapsulation was performed in an N_2 ambient glovebox chamber. Figure 2 depicts the fabrication flow diagram of the OLED lighting device.

Analysis method

The thickness of the PEDOT:PSS films coated on the substrate was measured using a spectral reflectance thickness measurement system (F32, Filmetrics Inc.). Atomic force microscope (AFM) system (NX 10, Park Systems Corp.) was used to measure the film surface roughness of the coated films. Intensity analysis of the OLED lighting

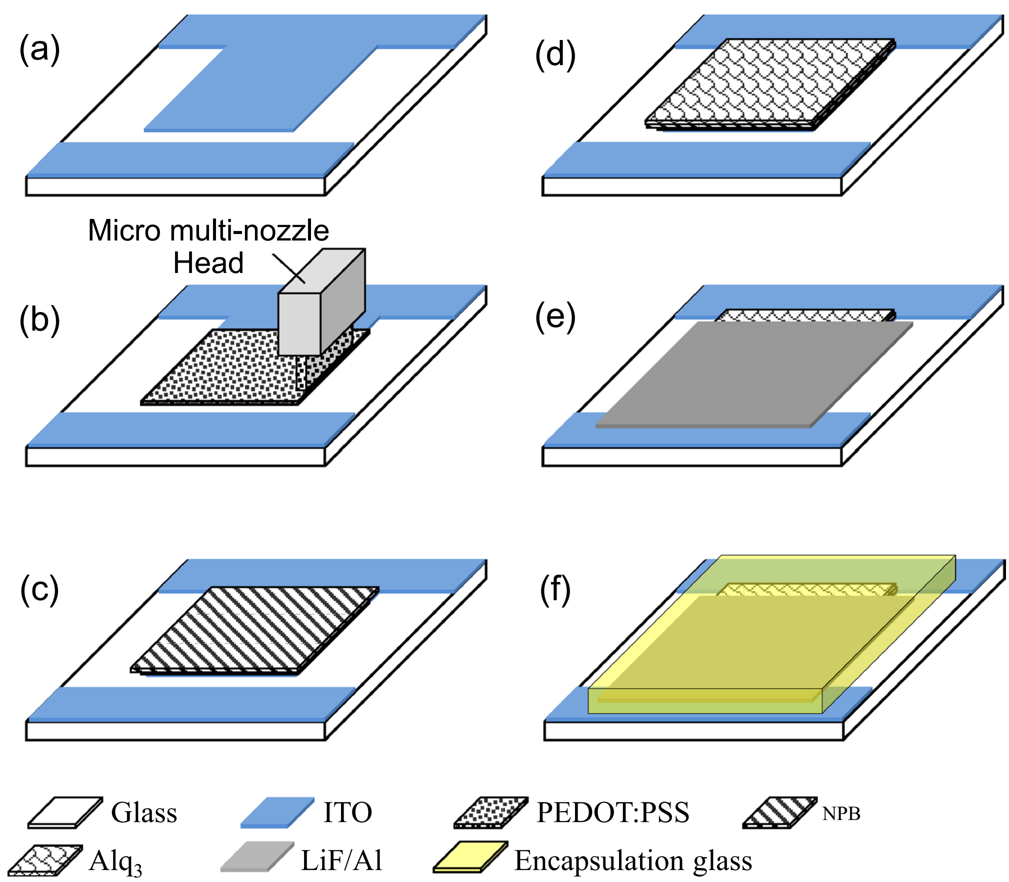

Fig. 2 The fabrication flow diagram of the OLED lighting device: **a** ITO electrode patterning, **b** PEDOT:PSS layer (HIL) coating using a micro multi-nozzle jet head, **c** NPB patterning, **d** Alq_3 patterning, **e** LiF/Al patterning, and **f** encapsulation

device was performed by ImageJ 1.53e software (NIH, USA). An OLED I-V-L Test System (M6100, McScience Co., Korea) was used to measure the current density, voltage, and luminance.

Results and discussion

μ-SN jet head and μ-MN jet head were fabricated by the procedure reported in our previous study [26, 27]. Figure 3a is a photograph of the micro single-nozzle jet head, and Fig. 3b shows schematic top and cross-sectional views on the μ-SN jet head corresponding to a red square in Fig. 3a. Jetting nozzles, suction channels, and inlets were formed on a silicon (Si) layer that is indicated by a dotted line in the top view illustration. As shown in the cross-sectional view illustration on the centerline (A – A') of Fig. 3b, the glass substrate with the outer holes was bonded by an anodic bonding system onto the Si substrate with the jetting nozzles and suction channels. Outer holes were formed on the glass substrate to prevent damage to the jetting nozzle during wiper cleaning. Figure 3c, d are SEM images of a jetting nozzle part and the magnified jetting nozzle and suction channel. μ-MN jet head has eighteen nozzles of 100 μm diameter arranged at 2 mm intervals and two suction channels were interconnected to the top side of the nozzle array [26, 27].

In the nozzle jet coating process, continuous stream jet flow generation is a very important step because the coating thickness is controlled by regulating the jetting pressure after the continuous stream jet flow is generated. Figure 4 shows sequential photographs of the continuous stream jet flow generated using the micro single-nozzle jet head. In our system, at a jetting pressure range of less than 10 kPa, nozzle jetting forms a dangling droplet at the nozzle tip, as shown in Fig. 4a. To generate the continuous stream jet flow, the dangling droplet should be removed by increasing the jetting time. However, when vacuum suction through the suction channel

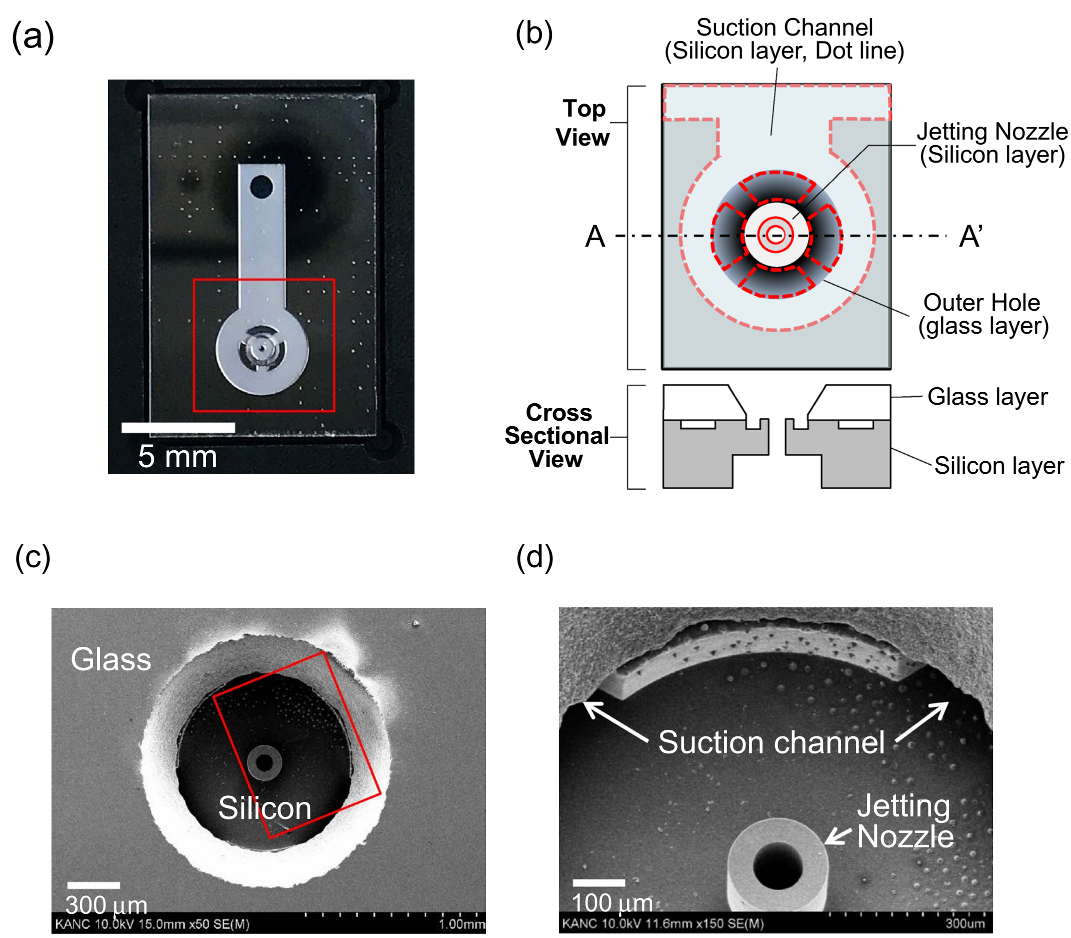

Fig. 3 Microfabrication results: **a** a photograph of the fabricated micro single-nozzle jet head (size: 10 mm × 15 mm), **b** a schematic illustration of part of a micro single-nozzle jet plate denoted by the red square in **a**, **c** SEM images of **c** a jetting nozzle part and **d** the enlarged jetting nozzle part indicated by the red square in **c**

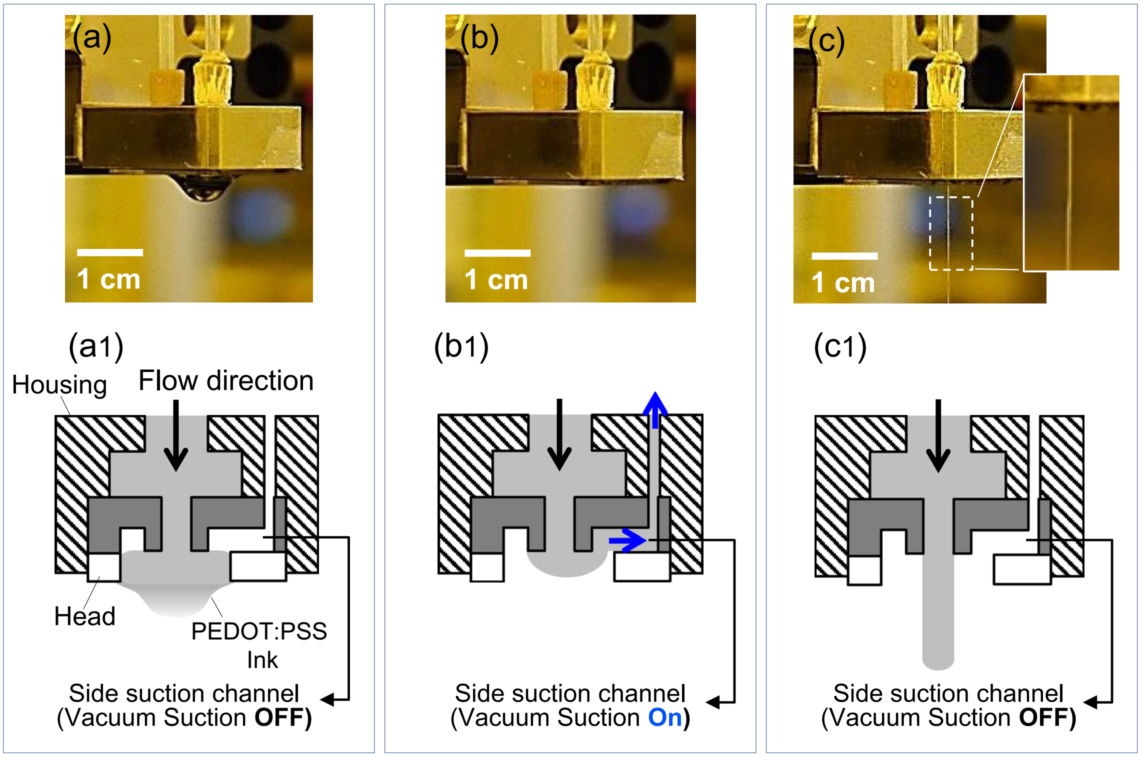

Fig. 4 Sequential photographs of the micro single-nozzle jetting by applying vacuum suction to the side of the jetting nozzle: **a**–**c** photograph images around the tip of a nozzle, **a1**–**c1** cross-sectional schematic diagram of jetting (modified from Shin et al. [23, 24])

was applied to the side of the jetting nozzle, the dangling droplet formation phenomenon was disappeared at the nozzle end, which interferes with the continuous stream jet flow [26, 27]. Figure 4b and c shows sequential photograph when the vacuum suction is applied to the side suction channel. Figure 4a1–c1 is a cross-sectional schematic diagram illustrating the jetting steps matched to photograph images of Fig. 4a–c. The continuous stream jet flow of the diluted PEDOT:PSS solution was formed by $P_{jetting} = 10$ kPa and $P_{suction} = 90$ kPa within 1 s (Fig. 4b and c). The stable continuous jet flow was maintained even after the suction pressure stopped.

Before applying the PEDOT:PSS thin film coating to fabricate the OLED lighting device, the thickness of PEDOT:PSS thin film was analyzed by changing the jetting pneumatic pressure of the μ-MN jet head. The all ITO-deposited glass substrate was exposed by an O_2 plasma system for 30 s to obtain the wetting surface for the diluted PEDOT:PSS solution. Figure 5 shows a clear decreasing trend in the contact angles with the surface treatment time. For the ITO-deposited glass, the contact angles decreased with increasing substrate surface treatment time for both deionized (D.I.) water and diluted PEDOT:PSS liquid. The initial contact angle of the D.I. water and the diluted PEDOT:PSS were 68.6 ± 1.9° and

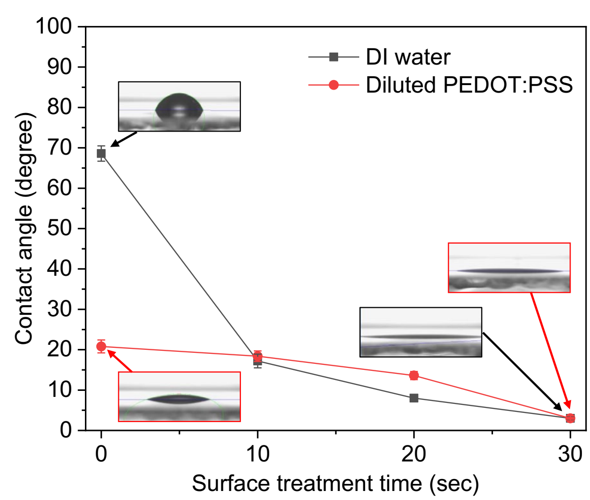

Fig. 5 Variation of contact angles of D.I. water and diluted PEDOT:PSS liquids on the ITO-deposited substrate with the O_2 plasma surface treatment time

20.8 ± 1.6°, respectively, but after O_2 plasma exposure for 30 s, their contact angles drastically diminished to less than 5°

Figure 6a shows a photograph of the continuous stream jet flow generated in the proposed method. The diluted PEDOT:PSS solution was jetted at jetting pneumatic pressure of 100, 120, 160, and 200 kPa, respectively ($V_{head} = 1$ m/s, $d_{head\text{-}subs} = \sim 1$ mm). As shown in Fig. 6a, among the total eighteen nozzles in the micro multi-nozzle head, twelve nozzles were used in the coating test, because single-path coating using twelve nozzles could deposit a PEDOT:PSS thin film pattern sufficient to cover the 20 mm × 20 mm emission area of the OLED lighting device fabricated for the feasibility test. The entire width of the single-coated pattern was about 36 mm, and the edge height of the single-path coated PEDOT:PSS pattern was approximately three times higher than that of a center area because of the coffee ring effect (Fig. 6b). The line profile of the single-coated PEDOT:PSS pattern was mapped by measuring thickness at 1 mm spacing using a spectral reflectance system.

Figure 6c shows the thickness analysis results on the PEDOT:PSS films coated by control of the jetting pneumatic pressure ($P_{jetting}$): (a) 100 kPa, (b) 120 kPa, (c) 160 kPa, and (d) 200 kPa. The thickness line profile of the single-coated PEDOT:PSS pattern was mapped measured at 1 mm intervals using the spectral reflectance thickness measurement system. The thickness of the coated PEDOT:PSS film was 16.45 ± 3.47 nm, 24.25 ± 1.55 nm, 28.00 ± 3.08 nm, and 29.34 ± 2.06 nm according to the jetting pressure, respectively. The film thickness and printed width increase with increasing jetting pressure. The most uniform thickness of the coated PEDOT:PSS thin film was 24.25 ± 1.55 nm at the jetting pressure of 120 kPa. In the thickness analysis, about 5 mm-wide coffee ring regions at both edges of the printed pattern were excluded because a 26 mm width excepting the coffee ring region is sufficient to coat a uniform PEDOT:PSS thin film for fabricating an OLED lighting device with 20 mm × 20 mm emission area, as mentioned above.

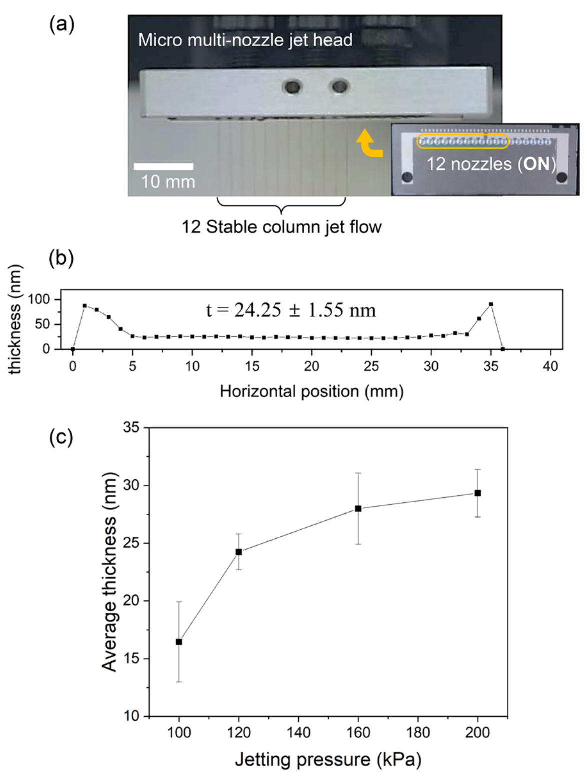

Fig. 6 **a** A photograph of continuous stream jet flow formation, **b** thickness profile of the single-path coated PEDOT:PSS pattern, **c** average thickness change of the single-path coated PEDOT:PSS films for the applied jetting pneumatic pressure of 100, 120, 160, and 200 kPa

We performed AFM and SEM analyses to investigate the surface topography change of the coated PEDOT:PSS film surface versus the bare ITO substrate surface. From the SEM analysis (Fig. 7a and b), it was confirmed that the clusters consisting of tens of nanometer grains disappeared from the ITO-deposited glass substrate after nozzle jet coating of PEDOT:PSS. In the AFM analysis (Fig. 7c and d), the root-mean-square roughness (R_{rms}) and peak-to-valley roughness ($R_{p\text{-}v}$) of bare ITO were measured as 1.52 nm and 16.49 nm, respectively, and the R_{rms} and $R_{p\text{-}v}$ values of the nozzle jet-coated PEDOT:PSS films were 0.90 nm and 7.55 nm. The R_{rms} and $R_{p\text{-}v}$ values of the nozzle jet-coated PEDOT:PSS film surface were significantly reduced compared to the bare ITO surface. An organic thin film with a fairly flat and smooth surface was obtained by the micro multi-nozzle jet coating method.

For the feasibility test, PEDOT:PSS films as an HIL were coated by μ-MN jet coating to fabricate an OLED lighting device with a 20 mm × 20 mm emission area, as illustrated in Fig. 2. The diluted PEDOT:PSS solution was coated through twelve micro nozzles for a target thickness of 24 nm. The jetting conditions were $P_{jetting} = 120$ kPa, $P_{suction} = 90$ kPa, $V_{head} = 1$ m/s and $d_{head\text{-}subs} = \sim 1$ mm. Fig. 8 shows a schematic illustration of the OLED lighting device structure (Fig. 8a) and a photograph image of the fabricated OLED lighting device (Fig. 8b). An emission test confirmed that the OLED lighting device was successfully fabricated without moiré patterns. This result shows that the PEDOT:PSS organic film can be uniformly coated by a μ-MN jet coating method, as predicted by the verification result from the AFM surface topography analysis (Fig. 7). Table 1 represents the summary of the OLED lighting device performance according to the coating methods reported in other previous researches [1, 3, 29–31]. Our OLED lighting device fabricated by a μ-MN jet coating method has superior device performance compared to

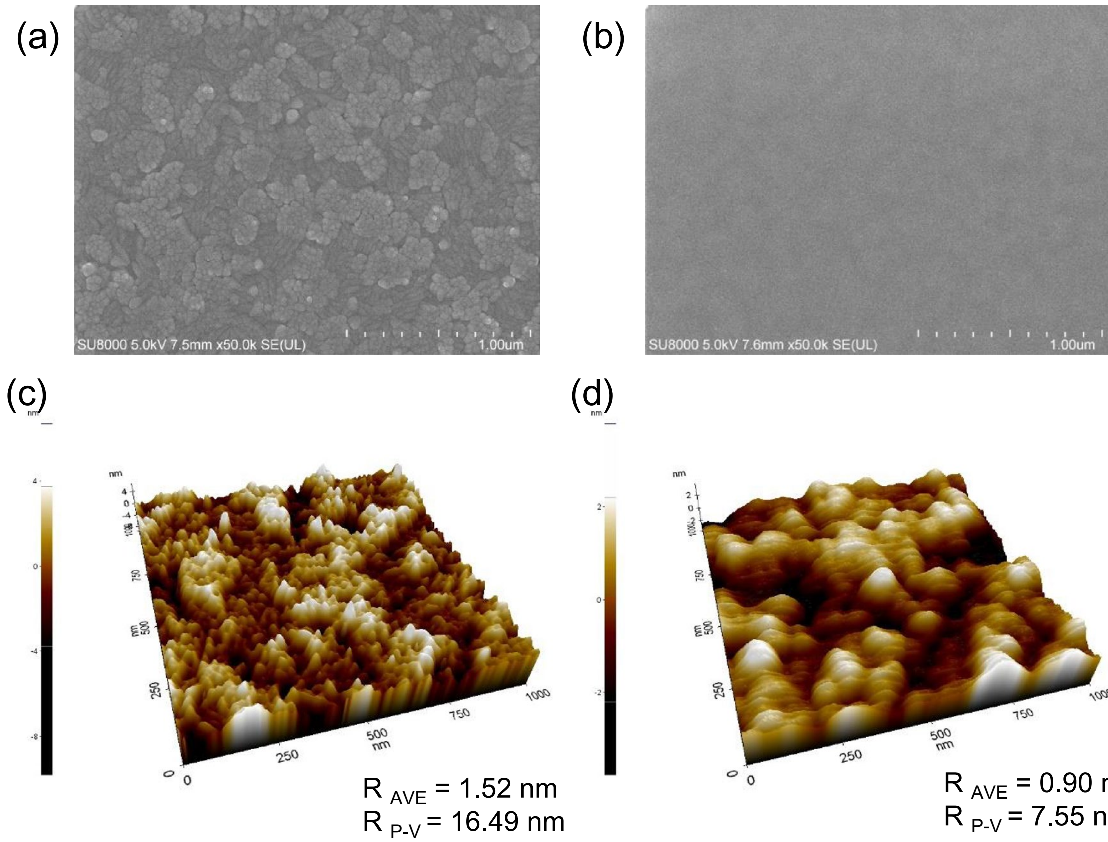

Fig. 7 Surface topography analysis results: SEM images of **a** a bare ITO-deposited glass surface and **b** PEDOT:PSS film surface deposited on the ITO-deposited glass by micro multi-nozzle jet coating, **c** AFM images of **a** a bare ITO-coated glass and **d** PEDOT:PSS film surface deposited on the ITO-deposited glass by micro multi-nozzle jet coating

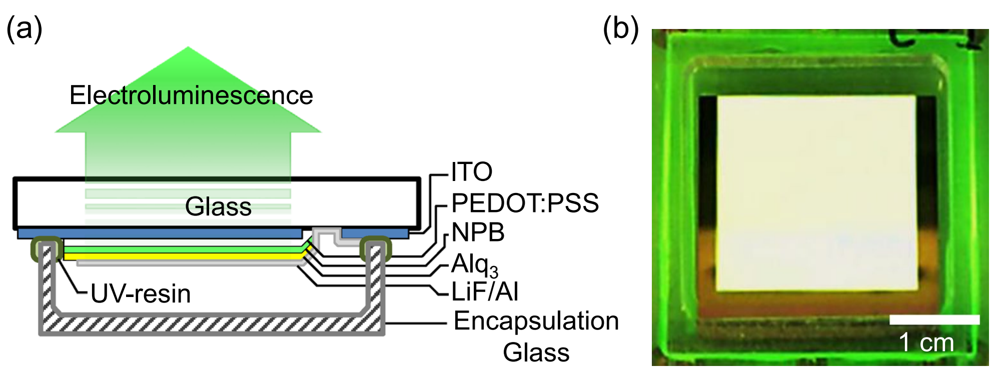

Fig. 8 **a** Schematic of the OLED lighting device, **b** photograph of the OLED lighting device with a 20 mm × 20 mm emission area (PEDOT:PSS deposited by micro multi-nozzle jet coating)

devices fabricated by other coating methods. The maximum luminance, current efficiency, and power efficiency were 10,125 cd/m^2 (@ 6.7 V), 63.7 cd/A (@ 4.3 V), and 46.5 lm/W (@ 4.1 V), respectively.

We also fabricated an OLED lighting device with a 70 mm × 70 mm emission area to investigate the large-area coating performance of μ-MN jet coating compared to μ-SN jet coating. To coat the HIL covering

Table 1 Summary of the OLED lighting device performance according to the coating methods (CE: current efficiency, PE: power efficiency)

No	Coating methods	Emission area for IVL measurement [mm × mm]	Luminance [cd/m^2]	Efficiency
1 [1]	Slot-die	2 × 2	-	PE: 28.7 lm/W
2 [3]	Slot-die	2 × 2	~ 19,500	PE: 27.2 lm/W
3 [29]	Slot-die	50 × 50	47,000	CE: 29 cd/A, PE: 14 lm/W
4 [30]	Slot-die	6 × 4	5200	CE: 31.3 cd/A, PE: 8.1 lm/W
5 [30]	Flexo printing	6 × 4	25,200	CE: 20.1 cd/A, PE: 5.8 lm/W
6 [31]	Blade-Jet	-	8930	PE: 8.42 lm/W
Our study	Nozzle jet	20 × 20	10,125	CE: 63.7 cd/A, PE: 46.5 lm/W

70 mm × 70 mm emission area, the diluted PEDOT:PSS was jetted by the μ-MN jet head moving with 22 mm print pitch where the print pitch is the interval that the stage travels perpendicular to the direction of head movement at a criterion of the head center point. An emission test was performed under 7.0 V driving. Since an auxiliary electrode was not used in this study, a luminance attenuation phenomenon occurred in the OLED lighting devices with a 70 mm × 70 mm emission area due to the lateral voltage drop caused by the resistance of the transparent ITO electrode, which limits the side current flow [32]. Therefore, to compare μ-MN jet coating and μ-SN jet coating, the luminescence images were analyzed in the horizontal direction. Figure 9a is a photograph of an

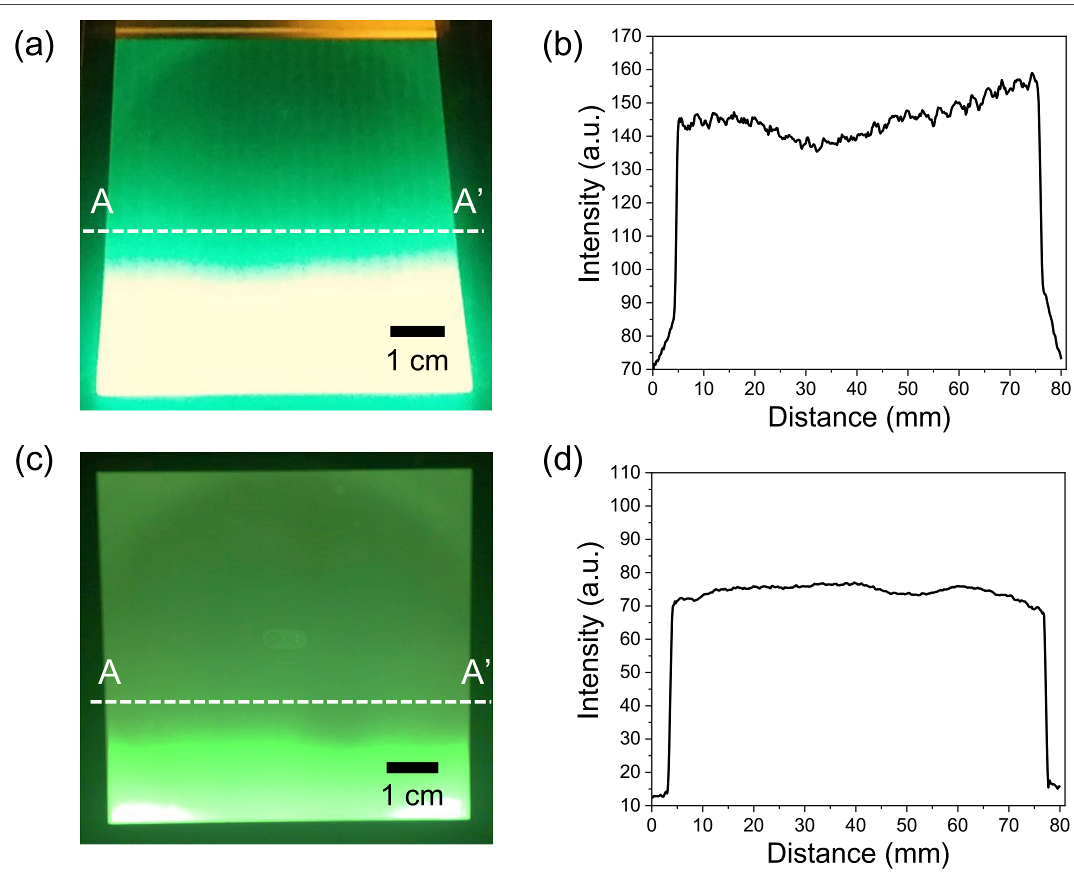

Fig. 9 Emission test and intensity analysis of OLED lighting device (70 mm × 70 mm emission area); **a** an emission image and **b** an intensity line profile for the OLED lighting device fabricated with the PEDOT:PSS thin film coated by the micro single-nozzle jet head, **c** an emission image and **d** an intensity line profile for the OLED lighting device fabricated with the PEDOT:PSS thin film coated by the micro multi-nozzle jet head

OLED device fabricated using a PEDOT:PSS layer coated by the μ-SN jet head. The intensity line profile of the dotted line (A–A′) on the luminescence image (Fig. 9b) showed stripe patterns, which can be caused by μ-SN jet coating trace, spread vertically from the top side to the bottom side. However, for the OLED device fabricated using a PEDOT:PSS layer coated by the μ-MN jet head, relatively homogenous luminescence without stripe patterns was observed, as shown in the luminescence image (Fig. 9c) and the intensity line profile (Fig. 9d). A large-area coating comparison study through the fabrication of OLED lighting devices with a 70 mm × 70 mm emission area showed that the μ-MN jet coating method is very useful for the organic thin film deposition process on large area flat substrates.

Conclusions

In this paper, we proposed an organic thin film deposition method for an OLED lighting device using μ-MN jet coating process. To demonstrate organic thin film deposition, a PEDOT:PSS solution diluted by EtOH with 90 vol% was used as the ink to deposit a hole injection layer of the OLED lighting device. The diluted PEDOT:PSS solution was coated at the conditions of were $V_{head} = 1$ m/s and $d_{head\text{-}subs} = \sim 1$ mm by changing the jetting pneumatic pressure. The PEDOT:PSS thin film was very uniformly coated at $P_{jetting} = 120$ kPa. For a 26 mm width excluding the coffee ring region, the average thickness the coated PEDOT:PSS thin film was 24.25 ± 1.55 nm and its uniformity (CV) was 6.39%. AFM analysis demonstrated that a PEDOT:PSS thin film with a fairly flat and smooth surface could be deposited by μ-MN jet coating method. R_{rms} and $R_{p\text{-}v}$ of the coated PEDOT:PSS film surface were significantly reduced compared to the bare ITO surface. To demonstrate the feasibility of the proposed μ-MN jet coating method, OLED lighting devices were fabricated by vacuum thermal evaporation of emission layers and metal electrodes after μ-MN jet coating of a PEDOT:PSS thin film (HIL). Single-path coating using twelve nozzles could deposit a PEDOT:PSS thin film pattern sufficient to cover the 20 mm × 20 mm emission area of the OLED lighting device, and thereby the OLED lighting device was successfully fabricated without moiré patterns. In a large-area coating comparison study between μ-SN jet coating and μ-MN jet coating, relatively homogenous luminescence was observed in the luminescence image and the intensity line profile for the OLED device fabricated by a μ-MN jet-coated PEDOT:PSS layer. However, the stripe pattern appeared in the emission test for the OLED lighting device fabricated with a μ-SN jet-coated PEDOT:PSS layer. These results support that the μ-MN jet coating method is very effective to deposit a uniform organic thin film for the solution-based large-area manufacturing of OLED lighting devices.

Acknowledgements
This study was conducted with supported by Ministry of Trade, Industry & Energy (MOTIE, No. 20010464).

Authors' contributions
KYS contributed to the optimization of the coating condition and fabrication of the multi-nozzle jet head. MK and KTK contributed to the fabrication of the OLED lighting device. KHC designed the fabrication process of the OLED lighting device. SHL supervised the research and wrote the overall manuscript. All authors read and approved the final manuscript.

Funding
Ministry of Trade, Industry & Energy (MOTIE), Project No. 20010464.

Availability of data and materials
Datasets supporting the conclusions of this article are included within the article.

Declarations

Ethics approval and consent to participate
Not applicable.

Consent for publication
Authors consent the SpringerOpen license agreement to publish the article.

Competing interests
The authors declare that they have no competing interests.

Author details
[1]Korea Institute of Industrial Technology, 143 Hanggaul-ro, Sangnok-gu, Ansan-si, Gyeonggi-do 15588, Republic of Korea. [2]Program in Nanoscience and Technology, Department of Transdisciplinary Studies, Graduate School of Convergence Science and Technology, Seoul National University, Gwanggyo-ro 145, Yeongtong-gu, Suwon-si, Gyeonggi-do 16229, Republic of Korea.

Received: 18 May 2021 Accepted: 28 October 2021
Published online: 17 December 2021

References
1. Choi K-J, Lee J-Y, Shin D-K, Park J (2016) Investigation on slot-die coating of hybrid material structure for OLED lightings. J Phys Chem Solids 95:119–128. https://doi.org/10.1016/j.jpcs.2016.04.006
2. Raupp SM, Merkleina L, Pathak LM, Scharfer P, Schabela W (2017) An experimental study on the reproducibility of different multilayer OLED materials processed by slot die coating. Chem Eng Sci 160:113–120. https://doi.org/10.1016/j.ces.2016.11.018
3. Choi K-J, Lee J-Y, Park J, Seo Y-S (2015) Multilayer slot-die coating of large-area organic light-emitting diodes. Org Electron 26:66–74. https://doi.org/10.1016/j.orgel.2015.07.025
4. Gorter H, Coenen MJJ, Slaats MWL, Ren M, Lu W, Kuijpers CJ, Groen WA (2013) Toward inkjet printing of small molecule organic light emitting diodes. Thin Solid Films 532:11–15. https://doi.org/10.1016/j.tsf.2013.01.041
5. Cao W, Li J, Chen H, Xue J (2014) Transparent electrodes for organic optoelectronic devices: a review. J Photonics Energy 4(1):040990–040991. https://doi.org/10.1117/1.JPE.4.040990
6. Forrest SR (2004) The path to ubiquitous and low-cost organic electronic appliances on plastic. Nature 428:911–918. https://doi.org/10.1038/nature02498
7. Espinos N, Hosel M, Angmo D, Krebs FC (2012) Solar cells with one-day energy payback for the factories of the future. Energy Environ Sci 5:5117–5132. https://doi.org/10.1039/C1EE02728J

8. Cao W, Xue J (2014) Recent progress in organic photovoltaics: device architecture and optical design. Energy Environ Sci 7:2123–2144. https://doi.org/10.1039/C4EE00260A
9. Kim DY, Han YJ, Choi J, Sakong C, Ju BK, Cho KH (2020) Inkjet printed quantum dot film formed by controlling surface wettability for blue-to-green color conversion. Org Electron 84:105814. https://doi.org/10.1016/j.orgel.2020.105814
10. Khan A, Rahman K, Kim DS, Choi KH (2012) Direct printing of copper conductive micro-tracks by multi-nozzle electrohydrodynamic inkjet printing process. J Mater Process Technol 212:700–706. https://doi.org/10.1016/j.jmatprotec.2011.10.024
11. Lee SH, Yun GY, Koh Y, Lee S-H, Kim Y-K (2013) Fabrication of a 3 dimensional dielectrophoresis electrode by a metal inkjet printing method. Micro Nano Syst Lett 1:5. https://doi.org/10.1186/2213-9621-1-5
12. da Costa TH, Choi JW (2020) Low-cost and customizable inkjet printing for microelectrodes fabrication. Micro Nano Syst Lett 8:2. https://doi.org/10.1186/s40486-020-0104-7
13. Sim S-M, Lee Y, Kang H-L, Shin Y-K, Lee S-H, Kim J-M (2016) Transmission line printed using silver nanoparticle ink on FR-4 and polyimide substrates. Micro Nano Syst Lett 4:7. https://doi.org/10.1186/s40486-016-0032-8
14. Wengeler L, Schmitt M, Peters K, Scharfer P, Schabel W (2013) Comparison of large scale coating techniques for organic and hybrid films in polymer based solar cells. Chem Eng Process 68:38–44. https://doi.org/10.1016/j.cep.2012.03.004
15. Krebs FC (2009) All solution roll-to-roll processed polymer solar cells free from indium-tin-oxide and vacuum coating steps. Org Electron 10:761–768. https://doi.org/10.1016/j.orgel.2009.03.009
16. Søndergaard RR, Hosel M, Krebs FC (2012) Roll-to-Roll fabrication of large area functional organic materials. J Polym Sci Part B Polym Phys 51:16–34. https://doi.org/10.1002/polb.23192
17. Carvalho MS, Kheshgi HS (2000) Low-flow limit in slot coating: Theory and experiments. AIChE J 46:1907–1917. https://doi.org/10.1002/aic.690461003
18. Chesterfield R, Johnson A, Lang C, Stainer M, Ziebarth J (2011) Solution-coating technology for AMOLED displays. Inf Disp Mag 27(1):24–30. https://doi.org/10.1002/j.2637496X.2011.tb00339.xt
19. Bhamidipati KL, Didari S, Harris TAL (2013) Slot die coating of polybenzimiazole based membranes at the air engulfment limit. J Power Sourc 239:382–392. https://doi.org/10.1016/j.jpowsour.2013.03.132
20. Larsen-Olsen TT, Andreasen B, Andersen TR, Bottiger APL, Bundgaard E, Norrman K, Andreasen JW, Jørgensen M, Krebs FC (2012) Simultaneous multilayer formation of the polymer solar cell stack using roll-to-roll double slot-die coating from water. Solar Energy Mater Solar Cells 97:22–27. https://doi.org/10.1016/j.solmat.2011.08.026
21. Chesterfield RJ, Frischknecht KD, Stainer M, Truong N (2009) Multinozzle printing: a cost-effective process for OLED display fabrication. SID Symp Dig 40:951–954. https://doi.org/10.1889/1.3256956
22. Kang M, Shin K-Y, Kim M-K, Sung D-H, Kang K, Cho K-H, Lee S-H (2014) Continuous jetting formation using micro-machined silicon nozzles for nozzle printing. IWFPE 2014 I-18.
23. O'Regan M (2008) Reducing AMOLED manufacturing costs. IMID/IDMC/ASIA DISPLAY '08 Digest: 27–29.
24. IHS: Ink-jet printing to finally become a mass production OLED production process in 2020, https://www.oled-info.com/ihs-ink-jet-printing-finally-become-mass-production-oled-production-process-2020.
25. Moro L, Hauf CR (2021) Large-scale manufacturing of polymer planarization layers. Inf Disp Mag 37(2):10–15. https://doi.org/10.1002/msid.1194
26. Shin K-Y, Kang K, Lee S-H (2020) Organic thin film coating by micro multinozzle jet method. SID Symp Dig 51:2089–2092. https://doi.org/10.1002/sdtp.14333
27. Shin K-Y, Kang M, Kim M-K, Jung KS, Yoo CS, Kang K, Lee SH (2021) Large area organic thin film coating using a micro multi-nozzle jet head with side suction channels. Int J Precis Eng Manuf Green Tech. 8:829–840. https://doi.org/10.1007/s40684-021-00334-7
28. Yoon DG, Kang M, Kim JB, Kang K (2018) Nozzle printed-PEDOT:PSS for organic light emitting diodes with various dilution rates of ethanol. Appl Sci 208(2):203. https://doi.org/10.3390/app8020203
29. Park B, Kwon OE, Yun SH, Jeon HG, Huh YH (2014) Organic semiconducting layers fabricated by selfmetered slot-die coating for solution-processable organic light-emitting devices. J Mater Chem C 2:8614–8621. https://doi.org/10.1039/C4TC00817K
30. Raupp S, Daume D, Tekoglu S, Merklein L, Lemmer U, Hernandez-Sosa G, Sauer HM, Dörsam E, Scharfer P, Schabel W (2017) Slot die coated and flexo printed highly efficient SMOLEDs. Adv Mater Technol 2:1600230–1600231. https://doi.org/10.1002/admt.201600230
31. Young Seok JY, Yang M (2016) A novel blade-jet coating method for achieving ultrathin, uniform film toward all-solution-processed large-area organic light-emitting diodes. Adv Mater Technol 1:1600029. https://doi.org/10.1002/admt.201600029
32. Neyts K, Marescaux M, Nieto AU (2006) Inhomogeneous luminance in organic light emitting diodes related to electrode resistivity. J Appl Phys 100:114513. https://doi.org/10.1063/1.2390552

Publisher's Note